

We are IntechOpen, the world's leading publisher of Open Access books Built by scientists, for scientists

6,900

Open access books available

186,000

International authors and editors

200M

Downloads

Our authors are among the

154

Countries delivered to

TOP 1%

most cited scientists

12.2%

Contributors from top 500 universities



WEB OF SCIENCE™

Selection of our books indexed in the Book Citation Index
in Web of Science™ Core Collection (BKCI)

Interested in publishing with us?
Contact book.department@intechopen.com

Numbers displayed above are based on latest data collected.
For more information visit www.intechopen.com



Synthesis of Carbon Nanomaterials in a Swirled Floating Catalytic Chemical Vapour Deposition Reactor for Continuous and Large Scale Production

Sunny E. Iyuke and Geoffrey S. Simate
*University of the Witwatersrand, Johannesburg
South Africa*

1. Introduction

Carbon nanotubes (CNTs), 'rediscovered' (Monthieux & Kuznetsov, 2006) by Iijima as a byproduct of fullerene synthesis (Iijima, 1991), have attracted enormous scientific and technological interest. Their myriad applications in various fields since their rediscovery are no longer debatable. However, their commercial applications still depend on large scale synthesis (several thousands of tons per year) and associated cost of production. Various methods have been developed for the production of CNTs (Dresselhaus et al., 2001; Agboola et al., 2007). However, the three very useful and widespread methodologies include arc discharge, laser ablation and chemical vapour deposition (CVD) (Robertson, 2004; Agboola et al., 2007). Two key requirements revealed in these methods are as follows, (i) a carbon source, and (ii) a heat source to achieve the desired operating temperature (See & Harris, 2007). In the arc discharge, CNTs are produced from carbon vapour generated by an electric arc discharge between two graphite electrodes (with or without catalysts), under an inert gas atmosphere (Journet et al., 1997; Lee et al., 2002; Agboola et al., 2007). In the laser ablation, a piece of graphite target is vapourised by laser irradiation under an inert atmosphere (Journet & Bernier, 1998; Paradise & Goswami, 2007). As for the technique of CVD, it involves the use of an energy source such as plasma, a resistive or inductive heater, or furnace to transfer energy to a gas phase carbon source in order to produce fullerenes, CNTs and other sp^2 -like nanostructures (Meyyappan, 2004). As would be expected, some of these methods are more effective than others. The arc-discharge, though it produces CNTs of high quality with fewer structural defects, uses high temperature of up to 1500°C, which makes it difficult to be scaled up for commercial purposes. On the other hand, laser vaporisation method is an expensive technique because it involves high purity graphite rods and high power lasers. At the moment, the CVD methodology (or variations thereof) is the only promising process for the production of CNTs on a reasonably large-scale compared to arc-discharge and laser vaporization methods (Coleman, 2008). In addition, the process tends to produce nanotubes with fewer impurities (catalyst particles, amorphous carbon and non-tubular fullerenes) compared to other techniques (Esawi & Farag, 2007). The variants of the CVD are as a result of the means by which chemical reactions are initiated, the type of

reactor used and the process conditions (Deshmukh et al., 2010). The CVD is simple, flexible and allows high specificity of single wall or multi wall nanotubes through appropriate selection of process parameters, e.g., metal catalysts, reaction temperature and flow rate of feed stock (Nolan et al., 1995; Agboola et al., 2007; Moisala et al., 2006). Recently, a swirled floating catalytic chemical vapour deposition (SFCCVD) reactor was developed with the aim of up-scaling the production capacity (Iyuke, 2007). The simplified schematic presentation of a SFCCVD is shown in Figure 1. Typically it consists of a vertical quartz or silica plug flow reactor inside a furnace. The upper end of the reactor is connected to a condenser which leads to two delivery cyclones where the CNTs produced are collected. Feed materials including carrier gases are uniformly blended with the aid of a swirled coiled mixer to give optimum catalyst-carbon source interaction.

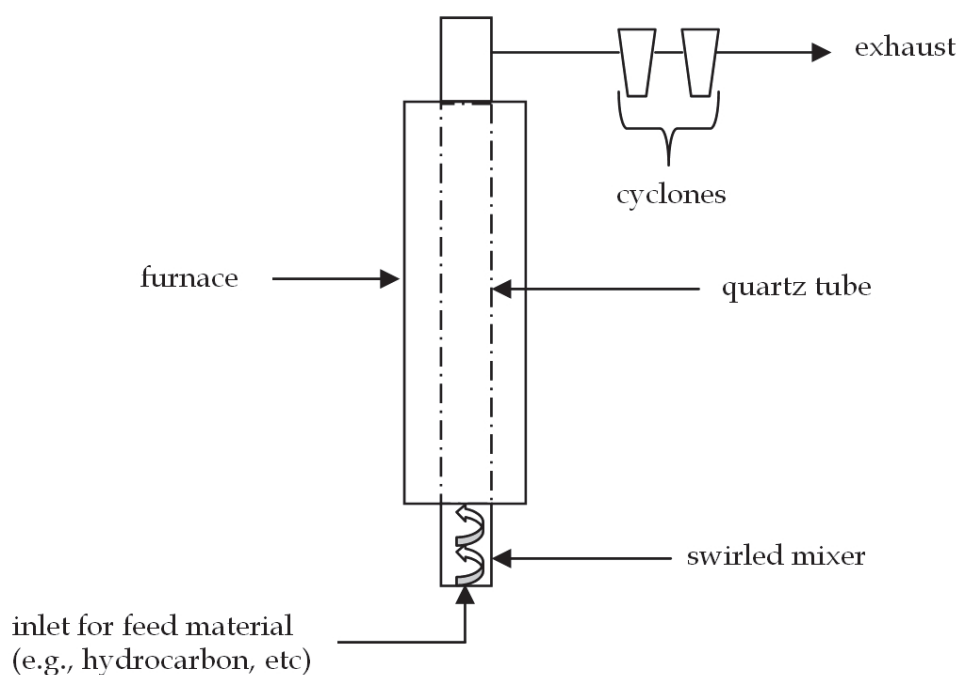


Fig. 1. Simplified schematic presentation of a swirled floating catalyst (or fluid) CVD

In this Chapter we discuss the continuous and large scale production of carbon nanomaterials in an SFCCVD reactor using various carbon sources. This reactor was found to be more successful than the microwave or the fixed-bed catalytic CVD modes (Iyuke et al., 2009). Furthermore, our large-scale synthesis method is simple and easily accessible to others with interest in this novel material. The chapter is divided into four themes covering, (1) the growth mechanisms and kinetics (section 2), (2) synthesis of both ordinary CNTs and carbon nanostructures (sections 3 and 4, respectively), (3) optimisation of the production (section 5), and (4) conclusions, challenges, and future prospects (section 6).

2. Growth mechanisms and kinetics

2.1 Growth mechanisms

Information on the mechanism of CNT growth, though important, is very scarce. As a result, more studies are needed to find out the characteristic mechanisms of CNT synthesis which may in turn guide the design and operation of continuous and large scale production of

carbon nanomaterials. Presently, various growth models based on experimental and quantitative studies have been proposed (Agboola et al., 2007).

One very important factor in the formation of CNTs through the CVD is the catalyst. Usually the vapor-liquid-solid (VLS) model is used to explain the growth of CNTs using catalysts (Saito, 1995). The catalyst acts as a seed for nucleation and growth by controlling the overall reaction with the hydrocarbon source (Yoon and Baik, 2001). The catalytic graphitisation (CG) of carbon sources to carbon nanomaterials is a sequential process that involves hydrocarbon decomposition, carbon dissolution, diffusion, adsorption and precipitation of carbon atoms to produce graphitised material (Yoon and Baik, 2001; Iyuke et al., 2007). However, the most accepted growth model suggests that after the decomposition of the carbon source, carbon diffuses into the metal particles until the solution becomes saturated. Carbon saturation in the metal occurs either by reaching the carbon solubility limit in the metal at a given temperature or by lowering the solubility limit via temperature decrease (Moisala et al., 2003). Supersaturation of the saturated solution then results in precipitation of solid carbon from the metal surface (Moisala et al., 2003; See and Harris, 2007). In summary, the mechanism of the catalytic growth of CNT or carbon nanofibre (CNF) is generally accepted as consisting of three steps (de Jong and Geus, 2000): The first step is the decomposition of carbon containing gases on the metal surface, with carbon atoms deposited on the surface. In the second step the carbon atoms dissolve in and diffuse through the bulk of the metal particles. It must be noted, however, that it is still unclear whether carbon atoms diffuse on the particle bulk (Ducati et al., 2004), on the particle surface (Hofmann et al., 2005), or whether surface and bulk diffusion compete. The final step is the precipitation of the carbon in the form of CNTs or CNFs at the other side of the catalyst particle.

The driving force for carbon diffusion and for the global process of carbon nanomaterial formation is the difference in solubility of carbon at the gas/catalyst interface and the catalyst/carbon nanomaterial interface, which is determined by the affinity for carbon formation of the gas phase and the thermodynamic properties of the carbon nanomaterial, respectively (Snoeck et al., 1997). The above mechanism shows that the steady state growth of CNT is a delicate balance between carbon source dissociation, carbon diffusion through the particle, and the rate of nucleation and formation of graphitic layers (Yu et al., 2005). This is illustrated by a simplified model shown in Figure 2. Tubule formation such as CNTs is favoured over other forms of carbon such as graphitic sheets with open edges. This is because a tube contains no dangling bonds and, therefore, is in a low energy form (Dai, 2001).

As illustrated in Figure 3, for the deposition of CNTs on a substrate, two general growth modes are known; the nanotubes can either follow a base-growth mode (A) or tip-growth mode (B) (Dai, 2001). Base-growth occurs when the catalyst remains anchored to the substrate, while tip-growth mechanism happens when the particle lifts off the substrate and is observed at the top of the CNTs. These growth modes depend on the contact forces or adhesion forces between the catalyst particle and the substrate (Leonhardt et al., 2006). While a weak contact favours tip-growth mechanism, a strong interaction promotes base-growth (Bower et al., 2000; Song et al., 2004).

However, Gohier et al. (2008) dispute the notion of adhesion forces between the catalyst particle and the substrate as controlling growth mechanism. Instead, they propose the catalyst particle size, and the 'carbon diffusion paths' during CNT nucleation as the main determinants for controlling the growth mechanism. Their results showed that for the same substrate/catalyst couples, single or few-wall CNTs follow the base-growth mechanism

while the tip-growth occurs only for the large multi-walled CNTs (MWCNTs). This behaviour was observed for three different catalysts commonly used in CNT synthesis, i.e., nickel, iron and cobalt. Besides the conventional explanation for growth mode change on catalyst/substrate interaction, Gohier and co-workers showed that growth mode can be explained by interaction between small carbon patches (polyaromatic carbon or reticulated carbon chains) and the catalyst. A strong interaction favours the formation of a graphene cap on the catalyst and leads to the single wall CNTs (SWCNTs) or few walls CNTs (FWCNT) growth via the base-growth mode. On the contrary, a weak interaction induces a diffusion of the graphitic section to the catalyst/substrate interface which drives the tip-growth mechanism.

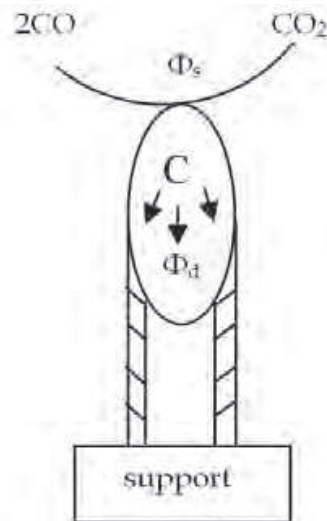


Fig. 2. Schematic representation of the CNT growth mechanism, where Φ_s represents surface decomposition rate, Φ_d means carbon diffusion rate. If $\Phi_s > \Phi_d$, encapsulating carbon forms on the catalyst surface; if $\Phi_s = \Phi_d$, the system is at balance and CNT grows at steady state (Yu et al., 2005).

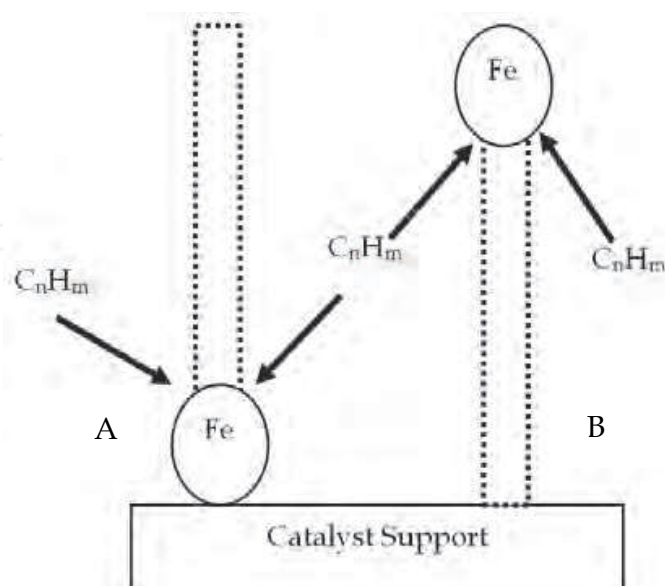
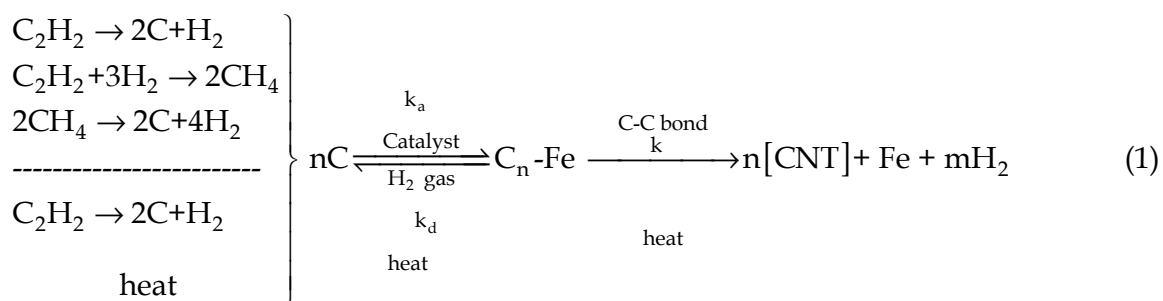


Fig. 3. General growth model (Dai, 2001)

Catalyst supports also play an important role. For example, in order to facilitate the large scale production of CNTs, support material should have a threefold action: minimises the formation of by-products (amorphous carbon, graphite nanospheres, etc), deters the aggregation of catalytic centres, and allows its removal from the resulting CNTs using simple chemical procedures (Tsoufis et al., 2007).

2.2 Kinetics

As already discussed mechanisms by which CVD occurs are very similar to those of heterogeneous catalysis; the reactant(s) adsorbs on the surface and then reacts on the surface to form a new surface (Fogler, 2006). Equation 1 represents the proposed mechanisms of catalytic graphitisation of a hydrocarbon (e.g., C_2H_2) to CNTs using a SFCCVD technique, whereby under heat the hydrocarbon and possibly the cracked fractions are dissociated into carbon atoms (Iyuke et al., 2007; Iyuke, 2007). The carbon atoms are deposited and adsorbed onto the catalyst (e.g., Fe) surface, which in turn react with each other to form C-C bonds thus producing graphene layers of CNTs produced.



Where the rate constants for the adsorption, desorption and reaction are k_a , k_d and k , respectively; m and n are stoichiometric coefficients.

The rate of CG (illustrated in Equation 1), can be written as a function of dissolution, adsorption and chemical reaction (Levenspiel, 1999; Iyuke et al., 2007).

$$r_{CG} = -r_{C_2H_2} = fn \text{ (dissolution, adsorption, chemical reaction)} \quad (2)$$

At appropriate temperature, where carbon nanomaterials grow, the dissolution of the hydrocarbon may be considered as complete, therefore, it becomes none rate limiting. As shown in Equation 1, the decomposed carbon atoms adsorb onto the catalyst surface, where adjacent carbon atoms react together to produce C-C bonds of graphene layers via a complex mechanism, which in turn produce carbon nanomaterials. Such complex mechanism can be expressed by rates of reactions catalysed by solid surfaces per unit mass as follows (Levenspiel, 1997; Iyuke and Ahmadun, 2002; Fogler, 2006):

$$-r_{C_2H_2} = \frac{1}{W_{cat}} \frac{dnC}{dt} = k\theta_C^n \quad (3)$$

Where W_{cat} is the weight of catalyst used, nC is the number of moles of carbon, superscript n is the order of the reaction, θ_C is the fraction of catalyst surface covered by carbon atoms (i.e., surface concentrations of adsorbed carbon, C), k is the reaction rate constant, and C is either carbon or other graphitised carbon nanoparticles. Therefore, Equation 3 is the rate of reaction occurring on the catalyst surfaces which is proportional to the concentration of

carbon (C) present on the surfaces or the fractions of surfaces covered by the carbon atoms of carbon nanomaterials (Iyuke et al., 2007). The commonly applied model, Langmuir-Hinshelwood, for reactions taking place between molecules or fragments of molecules adsorbed on the surface (Winterbottom and King, 1999) as shown in Equation 4 is adopted to obtain the reaction rate and equilibrium constant (Iyuke et al., 2007).

$$-r_{C_2H_2} = \frac{kC^n}{1+kC^n} \quad (4)$$

Equation 4 can be rearranged to give Equation 5.

$$\frac{1}{-r_{C_2H_2}} = \frac{1}{kC^n} + \frac{1}{k} \quad (5)$$

Using Equation 1, the exact model for the rate of reaction was developed below.



Equation 6 was modeled as:



Therefore, using the Langmuir-Hinshelwood mechanisms, the final model was obtained as,

$$r = \frac{kC_A^n \exp(1-\theta)}{k+1} \quad (8)$$

Where C_A is the concentration of reactant (e.g., C_2H_2), θ is the surface coverage, k is the reaction rate constant which is proportional to the diffusion coefficient of carbon (Kim et al., 2005), n is the order of reaction, t is the time of reaction.

Using experimental data the value of $n = 4$ was obtained from a plot of $1/-r_{C_2H_2}$ versus $1/C^n$ in Equation 5 (Iyuke et al., 2007). Consequently, the model in Equation 8 was used to predict the rate of production of CNTs at various temperatures and acetylene concentrations, and the results were compared to the experimental data (Table 1). Experimental data and results from the predictive model show reasonable agreement, with correlation coefficient ranging from 0.81 to 0.99 at various temperatures. The model equation is, therefore, able to represent data for SFCCVD technique in the production of CNTs. Both the experimental and predictive model results show that the concentration of acetylene and reaction temperatures affect the rate of CNT production.

Acetylene Concentration (ppm)	CNT production rate (mg/s); experimental versus computed			
	950°C	1000°C	1050°C	1100°C
1985	1.6(1.2)	2.7(1.9)	2.5(1.8)	2.1(1.9)
2728	2.8(3.0)	3.1(3.0)	4.3(3.0)	4.2(3.0)
3379	3.0(4.7)	4.0(4.7)	4.9(4.7)	3.8(4.7)
4058	4.5(5.8)	4.8(5.8)	4.2(5.8)	5.1(5.8)

Table 1. Experimental and computed production rate of CNTs at different temperatures (Iyuke et al., 2007).

3. Synthesis of ordinary carbon nanotubes

The production of CNTs in terms of the type and quality (for example) is controlled by several factors including carbon source. The commonly used gaseous carbon sources include carbon monoxide (CO) and hydrocarbon feed stocks such as methane, acetylene, ethylene, and n-hexane (Agboola et al., 2007). More recently, carbon dioxide (CO₂) has also been used in the synthesis of these carbon nanomaterials (Simate et al., 2010). There are typically two forms of CNTs according to the number of rolled up graphene layers that form the tube (as illustrated in Figure 4), i.e., SWCNTs and MWCNTs. A SWCNT is a graphene sheet rolled-over into a cylinder with typical diameter of the order of 1.2-1.4nm in magnitude (Journet and Bernier, 1998), while a MWCNT consists of concentric cylinders with an interlayer spacing of about 0.34nm (3.4Å) and a diameter typically of the order of 10-20 nm in magnitude (Dai, 2002).

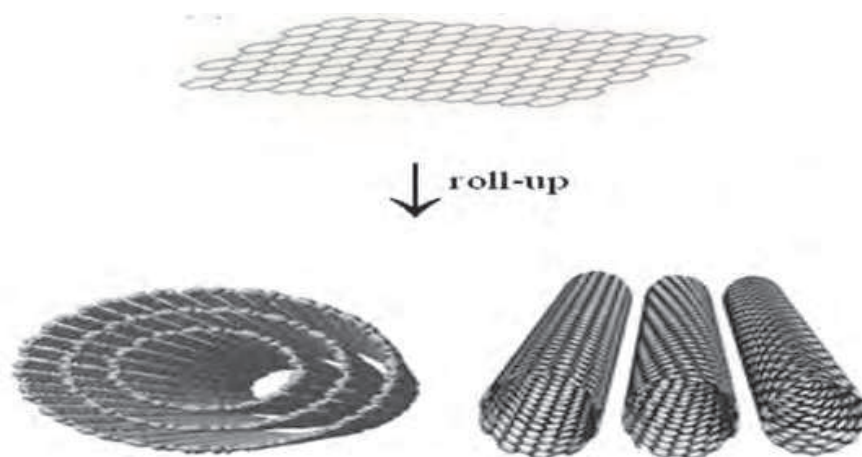


Fig. 4. Models and representation of multi-walled CNT and single-walled CNT (Merkoci, 2006; Liu, 2008).

In addition, there are two models which can be used to describe the structures of MWCNT. In the Russian doll model, a certain number of SWCNT with growing diameters are arranged in concentric cylinders. In the parachute model, a single graphite sheet is rolled in around itself. In MWCNTs, the nanotubes are typically bound together by strong van der Waals interaction forces and form tight bundles (Dai, 2002).

It seems likely that two different mechanisms operate during the growth of MWCNTs and SWCNTs, because the presence of a catalyst is absolutely necessary for the growth of the later (Ajayan, 2000). Furthermore, a key factor of CNT growth is the kinetics of carbon supply. An over-supply of carbon causes the formation of MWCNT rather than SWCNT because excess carbon activity allows the nucleation of extra nanotube walls (Wood et al., 2007). The stability of the double shell MWCNT is higher than SWCNTs on their own as the number of atoms increase (Sinnott et al., 1999). This is because the van der Waals interactions between the shells in the MWCNT increase as the nanotube gets longer. It is also observed that there is little difference in the stability of MWCNTs as a function of the helical arrangements of the shells (Sinnott et al., 1999). Compared to MWCNTs, one of the most significant features of SWCNT is the uniformity of size and the relative lack of any defects in the later. This explains the fact that methods to produce SWCNTs in significant large quantities developed rather quickly.

3.1 Use of acetylene

Acetylene has been the most widely used hydrocarbon in the production of CNTs by many researchers. Acetylene is more reactive than other hydrocarbons at the same reaction temperature, leading to CNTs of good quality and probably hinders the formation of carbon nanoshells which poison catalytic centres (Soneda et al., 2002). Furthermore, even molecular beam experiments have shown that acetylene is the most active growth precursor (Eres et al., 2005), and that it is the primary growth precursor in both hydrocarbon and alcohol feed stocks (Xiang et al., 2009; Zhong et al., 2009). Here, we discuss the results of using acetylene carbon source and organo-metallic ferrocene catalyst. Ferrocene was found to be a better catalyst precursor in the studied conditions since iron pentacarbonyl decomposes at lower temperatures resulting in the excessive growth of catalyst particles. Furthermore, its other advantages as an iron precursor include its innocuity and low cost (Barreiro et al., 2006).

The CNTs (and other nanomaterials to be discussed in section 4.1) were synthesized in a mixture of gases of acetylene, hydrogen and argon at the substrate temperature of 900-1050°C. Figure 5 shows typical transmission electron microscopy (TEM) images of CNTs grown in the temperature range of 1000 - 1050°C. The images reveal that each of the structures is hollow with inner diameter and length of several nanometers which confirm the presence of CNTs (Afolabi et al., 2007).

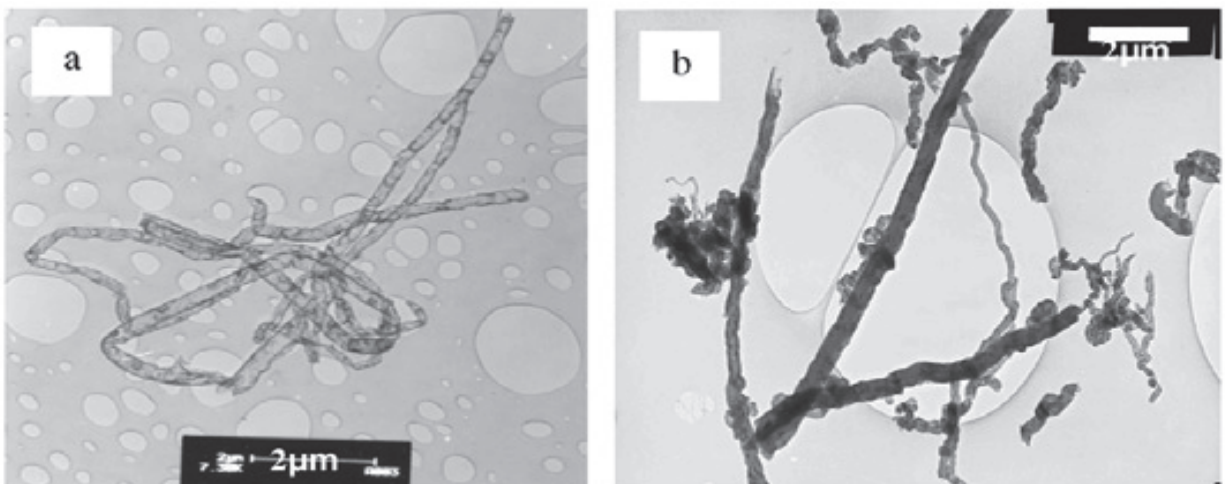


Fig. 5. TEM images of pure CNTs produced at (a) 1000°C and (b) 1050°C (Afolabi et al., 2007).

The diameter distribution of the CNTs based on the measurements from the sufficiently enlarged TEM images (results not shown in this Chapter) indicated that the diameter of the CNTs increased with increase in temperature (Afolabi et al., 2007). This was attributed to high rate of acetylene decomposition which maximised carbon generation leading to more CNT wall formation (Kumar and Ando, 2005; Afolabi et al., 2007).

The X-ray diffraction (XRD) pattern of the sample (Figure 6) reveals the characteristic pattern of graphitised carbon. The graphitic line (002) of this sample was observed at diffraction peak of 25.8° corresponding to inter-planer spacing of about 0.343 nm which is usually attributed to CNTs. This pattern also indicates high degree of crystallinity which suggest low content of amorphous carbon and impurities from catalysts (Afolabi et al., 2007). This observation is a marked difference from the results of many other CVD processes where impurities from catalyst employed in the pyrolysis process are always associated with the CNTs such that they have to be removed through various purification processes.

These multi-step purification processes can destroy the product. It is suggested that effective utilisation of the ferrocene catalyst during the decomposition process could have been responsible for the low content of iron impurities in the CNTs (Afolabi et al., 2007).

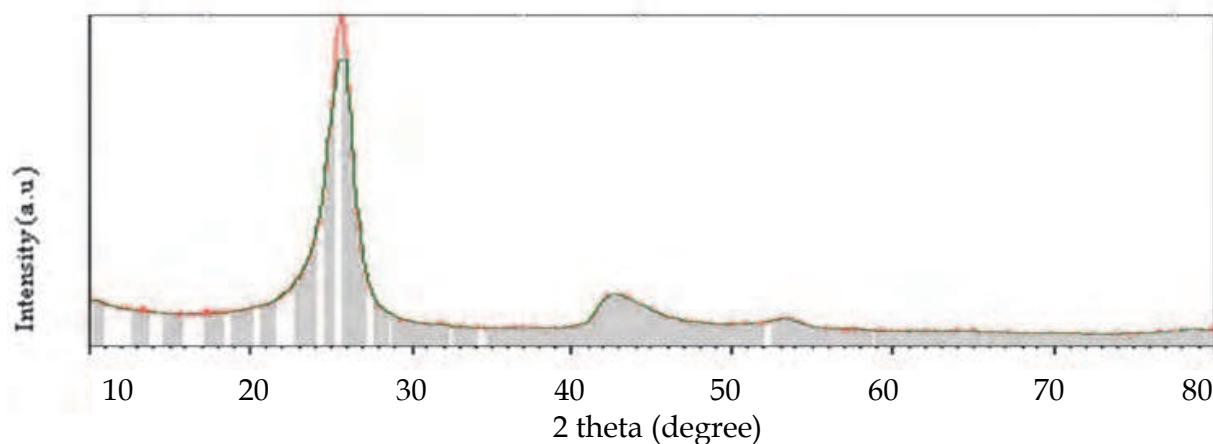


Fig. 6. XRD pattern of raw CNTs sample (Afolabi et al., 2007)

Table 2 shows the compositions of carbon nanomaterials at various conditions. These results indicate that accurate regulation of carbon source flow rate, hydrogen flow rate and temperature, which is a simple and versatile method, enables selective synthesis of various types of carbon nanomaterials. As can be seen from Table 2, CNTs were predominantly produced at very high temperatures (1000-1050°C). However, at temperatures above 1100°C there was decrease in production rate (Iyuke et al., 2007). The reduction in production at high temperature might have been due to the deactivation of the catalyst by carburization (Yamada et al., 2008) or sintering (Amama et al., 2009). Furthermore, low values of amorphous carbon were observed as the temperature increased as a result of amorphous carbon burning off at high temperatures (Iyuke et al., 2007).

Gas flow rate (mlmin ⁻¹)		Carbon nanomaterials at various temperatures (°C)			
Hydrogen	Acetylene	900	950	1000	1050
118	181	CNBas+CNTs	CNBas+CNTs	CNTs	CNTs
118	248	CNBas+CNTs	CNTs	CNTs	CNTs
118	308	CNBas+CNTs	CNTs	CNTs	CNTs
118	370	CNBas	CNTs	CNTs	CNTs
181	370	CNBas	CNTs	CNTs	CNTs
248	370	CNBas	CNTs	CNTs	CNTs

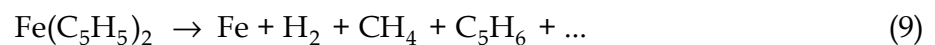
Table 2. Compositions of carbon nanomaterials at various conditions (Afolabi et al., 2007)

Similar studies on the SFCCVD reactor in the absence of hydrogen gas showed the production of CNTs and several other carbon nanomaterials at lower temperatures of 750°C to 900°C (Iyuke et al., 2009). For example, (1) a mixture of carbon nanoballs (CNBas), MWCNTs and CNFs at 750°C, (2) MWCNTs at 800°C, (3) a mixture of MWCNTs, SWCNTs and helical carbon nanofibres (HCNF) at 850°C, and (4) large quantities of HCNFs and strands of bamboo-like CNTs at 900°C. These results are different from the ones shown in Table 1 where high temperatures were needed for the production of carbon nanomaterials.

This can be attributed to the suppressing effect of hydrogen on the production of CNTs. The suppressing phenomenon was observed by several researchers as reviewed by Simate et al. (2010). The suppressing effect is due to the surface dehydrogenation of carbon to form methane. In fact, it has been observed that the presence of hydrogen can either accelerate or suppress the synthesis of CNTs (Yang and Yang, 1986; Endo, 1988; Ci et al., 2001) depending on the thermodynamics (Ci et al., 2001).

3.2 Use of ferrocene

This was an attempt to explore the use of organometallic complexes in the synthesis of CNT and other carbon nanomaterials. In particular, we explored the use of ferrocene both as a carbon source and the ‘carrier’ of elements to catalyst sites in CNT synthesis in our reactor. At a temperature above 500°C, ferrocene decomposes as given in Equation 9 (Leonhardt et al., 2006), and its unimolecular gas-phase decomposition is given in Equation 10 (Lewis and Smith, 1984).



This means that at a temperature higher than 500°C, solid or liquid-like iron particles and different kinds of hydrocarbons exist in the reaction zone of the SFCCVD equipment. Upon these particles, acting as catalyst nuclei, CNTs nucleate and grow with the carbon atoms provided solely by the ferrocene. This means that thermal decomposition of ferrocene provides both catalytic particles and carbon sources.

We investigated the production of CNTs from 800°C to 950°C by flowing a gas mixture consisting of argon and sublimated gaseous ferrocene through the reactor. Results showed that CNTs could be produced at all the temperatures with no significant difference in the amount of CNTs produced (i.e., $p > 0.05$). However, at higher reaction temperatures, there was less adherence of the product to the walls of the reactor. Therefore, for industrial processes, higher temperatures would need to be used.

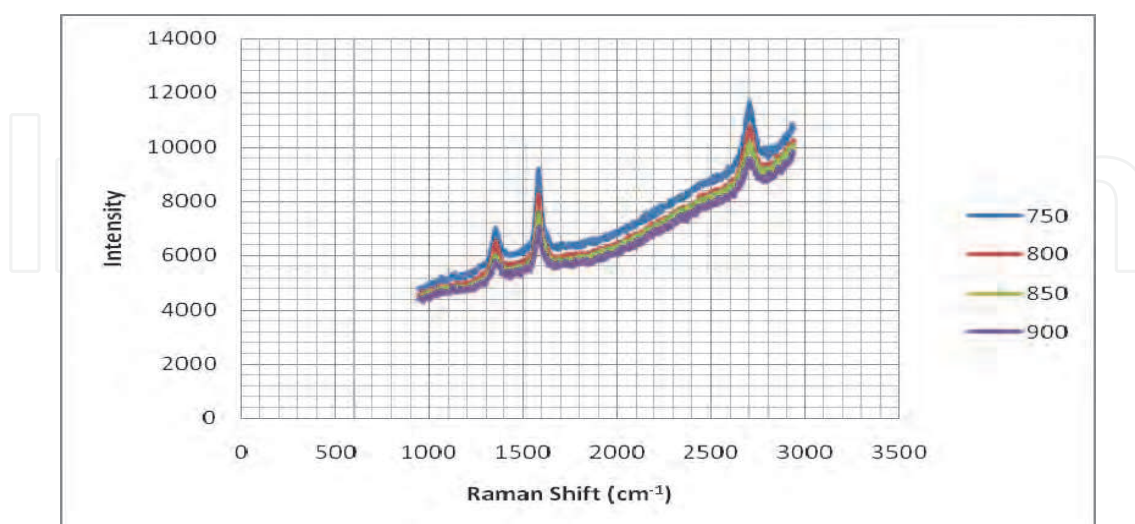


Fig. 7. Raman Shifts for the Products formed at different temperatures.

In contrast to results obtained by Barreiro and co-workers (Barreiro et al., 2006), where they predominantly produced SWCNT in a higher pressure horizontal CVD reactor using only

ferrocene, the Raman spectroscopy of our samples showed that MWCNTs were produced as shown in Figure 7. As can be seen from the figure, the Raman spectra of CNTs produced show similar intensities for both the dispersive disorder-induced D-band (1353.1 cm^{-1}) and its second-order related harmonic G-band (1580.3 cm^{-1}). This strongly supports the fact that MWCNTs were produced.

3.3 Use of xylene/ferrocene mixture

This section reports the continuous and large scale production of MWCNTs from xylene/ferrocene mixture in the presence or absence of hydrogen (Yah et al., 2011). Xylene was used as the solvent for the catalyst and also acted as the main carbon source. In other words, xylene was used as a solvent to dissolve the ferrocene for easy transportation into the reactor and also functioned as a CNT growth promoter. It was selected as the hydrocarbon source since it boils (boiling point $\approx 140^\circ\text{C}$) below the decomposition temperature of ferrocene ($\approx 190^\circ\text{C}$).

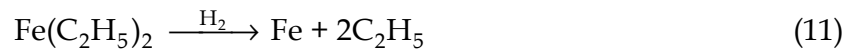
Just like other work already described, it was found that an increase in temperature increased the amount of CNTs produced (Table 3). While at 800°C there were no CNTs produced, (other than amorphous carbon) a very small amount of CNT was produced at 850°C . The non-production of CNTs at low temperatures (i.e., $< 850^\circ\text{C}$), was due to the low diffusion rates of iron and carbon which prevented the CNTs from nucleating and growing from the iron particles, but resulted in the formation of amorphous carbon (Kunadian et al., 2008). This implies that below 850°C , the production of CNTs from xylene/ferrocene mixture is unfavourable. However, above 1000°C there was a decrease in the amount of CNTs produced as a result of short reaction time caused by the deactivation of catalyst sites which occurs at such high temperature (Yu et al., 2005).

The present findings showed that between 900 and 1000°C , with an optimal production at 950°C (Table 3), MWCNTs were well aligned. This differs from earlier reports by Jacques et al. (2000) where they also described the production of MWCNTs at 725 - 775°C , with an optimal production at 725°C . Their product had more nanoball-like (100 nm long) structures at 750°C . Our results were similar to those previously reported by Vivekchand et al. (2004) where they produced MWCNTs from the mixture of xylene and ferrocene by pyrolysis at furnace temperature in the range of 800 - 1000°C .

Reactor Conditions	800°C	850°C	900°C	950°C	1000°C	950°C (double reactor feed volume)	950°C (1:7 H_2 :Ar carrier gas feed)
Observable number of CNTs per Cu grid square	0	2	8	16	13	18	47

Table 3. Effect of temperature on the amount of CNT formed (Yah et al., 2011).

With the introduction of hydrogen as one of the carrier gases, the amount of CNTs produced increased in the reactor by more than twice the amount produced at double reactor volume feed (see Table 3). Kunadian et al. (2008) also made similar observation when they prepared MWCNTs from xylene using the fixed bed CVD mode. This is because hydrogen has a strong influence in the gas-phase decomposition rate of ferrocene (Equation 11). This is an accelerating effect of hydrogen as stated in section 3.1.



In the absence of hydrogen, ferrocene dissociation does not occur until about 1100-1200 K, while its reduction occurs at temperatures as low as 673 K in the presence of hydrogen (Kuwana and Saito, 2007).

3.4 Use of acetylene and xylene/ferrocene mixture

This experimental work employed acetylene as the carbon source, hydrogen as a carrier gas, ferrocene dissolved in xylene as the catalyst precursor and the reactor operated from 900-1100°C in order to produce CNTs on a continuous basis. The results showed that CNTs produced at high ferrocene concentrations were riddled with high levels of iron impurities, while those at low ferrocene had only small traces of iron impurities. This was attributed to the limitation in the solubility of ferrocene in xylene at room temperature (Liu et al., 2002). In fact, Liu et al. (2002) observed that at low ferrocene concentrations, the catalysis efficiency of ferrocene is high. Though the quantity of CNTs produced at lower ferrocene concentrations was small, the low amorphous carbon and iron particles in the samples resulted in the formation of clean CNTs.

3.5 Use of carbon dioxide and methane

Though the pyrolysis of hydrocarbon precursors for synthesizing CNTs is very useful and is used widely, there are some disadvantages associated with these methods. Most hydrocarbons used in these methods are hazardous chemicals, and for most cases, the pyrolysis temperatures are around 1000°C, which are impractical for large scale industrial production (Qian et al., 2006). One approach to tackling this problem is by the use of CO₂ which is a cheap, non-toxic, low-energy, and abundant molecule on the earth (Qian et al., 2006). The CO₂ is easily formed by the oxidation of organic molecules during combustion or respiration. Furthermore, CO₂ can be acquired from natural reservoirs or recovered as a by-product of industrial chemical processes, so, no new production of CO₂ is necessary and there will be no addition to greenhouse gases (Young et al., 2000).

This work presents the successful production of CNTs and CNFs by catalytic decomposition of methane (CH₄) and CO₂ over an unsupported nickel alloy catalyst (LaNi₅) in a 'modified' SFCCVD reactor (Figure 8) at temperatures ranging from 650-850°C (Moothi, 2009; Maphutha, 2009).

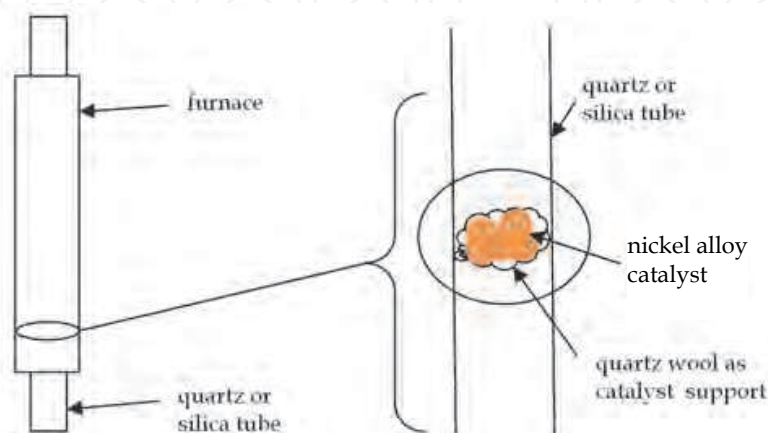


Fig. 8. Modified SFCCVD by attaching quartz wool as support for unsupported catalyst.

It was observed that CH_4 produced well defined CNTs at all the tested temperatures (650–850°C) as shown in Figure 9. A mixture of CNFs and CNTs was produced at lower temperatures (650–700°C) using CO_2 , whereas at higher temperatures (750–850°C) only CNFs were produced as shown in Figure 10. The CNFs are cylindric nanostructures with graphene layers arranged as stacked cones, cups or plates. Furthermore, CNFs with graphene layers wrapped into perfect cylinders are called CNTs. In summary, this work has shown that the LaNi_5 catalyst is capable of decomposing CO_2 into CO and CNTs both of which are useful compounds. The CNTs produced are not entangled like other catalysts making it easier to separate them for further studies or used as nano-resistors.

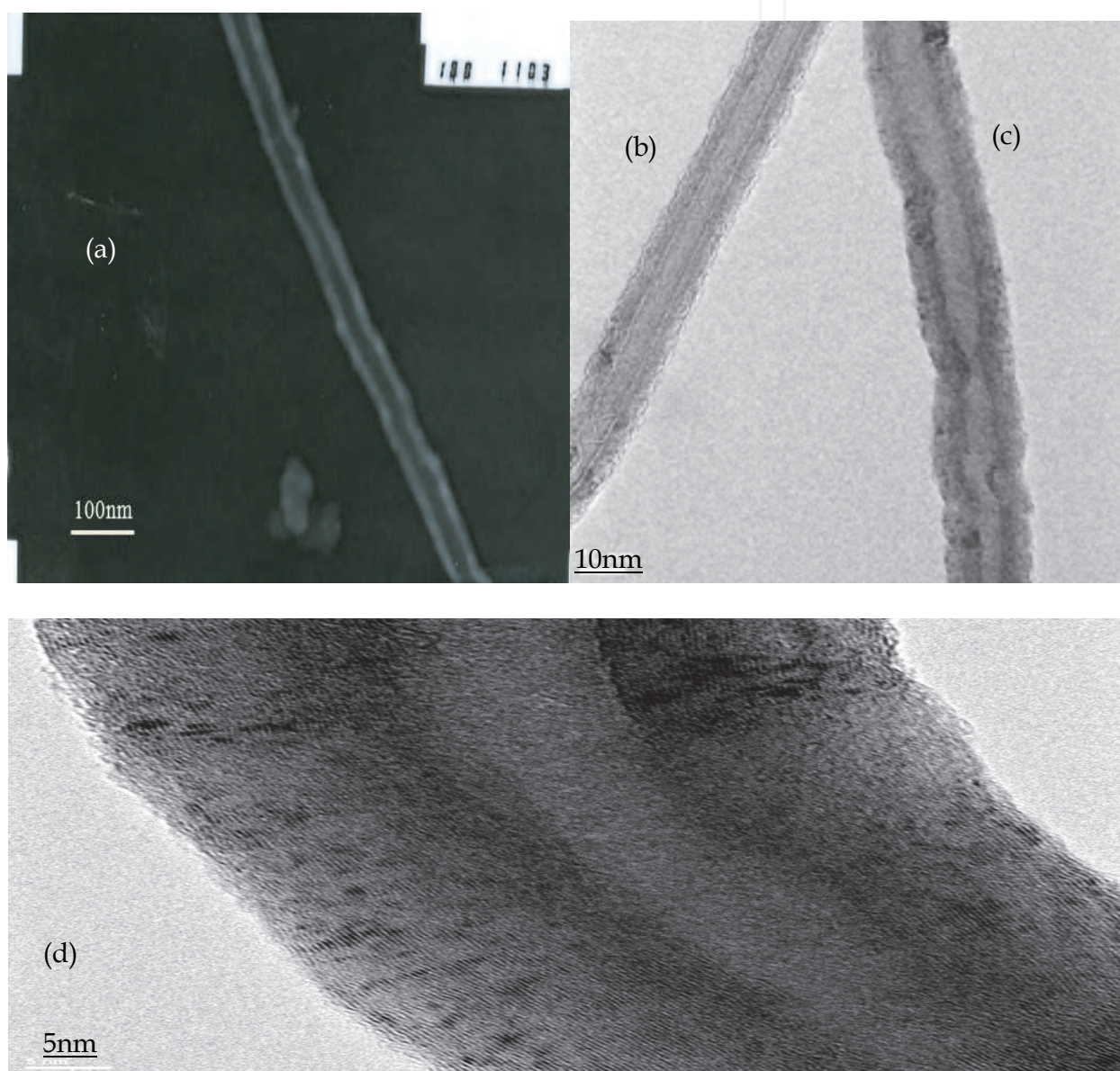


Fig. 9. (a) CNT produced at 650°C, (b) CNT produced at 750°C, with inside diameter and outside diameter of 6.6 nm and 16.6 nm, respectively (c) CNT produced at 750°C, with inside diameter and outside diameter of 10 nm and 23.2 nm, respectively, and (d) CNT produced at 850°C (Moothi, 2009; Maphutha, 2009)

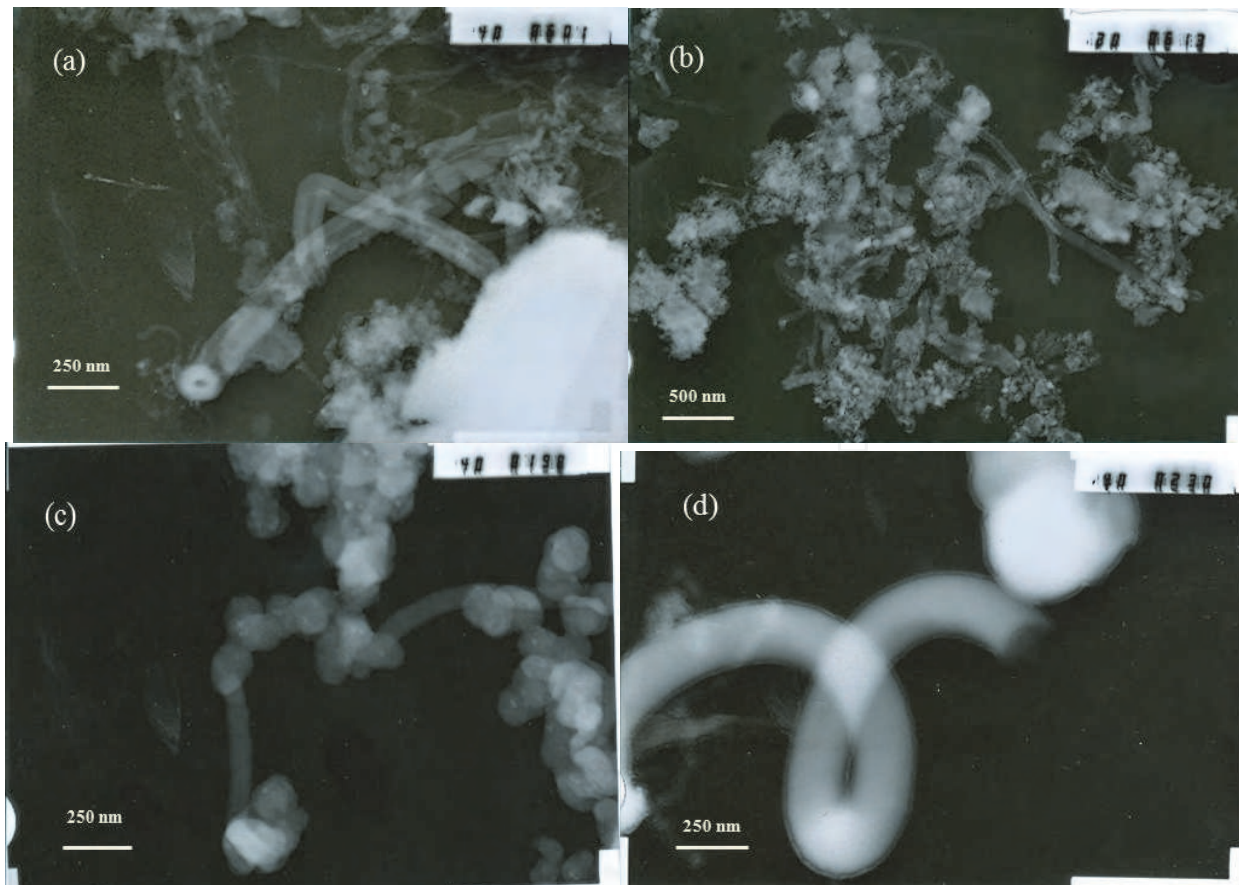


Fig. 10. (a) CNF/CNT produced at 650°C, growing from the large catalyst particles, (b) CNF/CNT produced at 700°C, (c) CNF produced at 750°C, with catalyst particles attached at ends, and (d) CNF produced at 850°C, with a circular structure and no catalyst embedded (Moothi, 2009; Maphutha, 2009)

4. Synthesis of other carbon nanostructures

As alluded to earlier, the nature of carbon nanomaterials produced by CVD method including SFCCVD depends on the working conditions such as temperature and pressure of operation, the volume and concentration of carbon source, the size and pretreatment of metallic catalysts, and the time of reaction (Paradise and Goswami, 2006). As a result, in the ambit of CNT production several other carbon nanomaterials may be produced in the CVD depending on the conditions. Some of these nanomaterials are CNBas (Zhong et al., 2000), CNFs (Endo et al., 2001), carbon nanorods (Liu et al., 2000) and even diamond particles (Zhang et al., 2006; Afolabi et al., 2009).

4.1 Carbon nanoballs

The CNBas are a group of shaped carbon materials with a spherical or near spherical shapes under 100 nm diameter. They include balls, spheres, microbeads, carbon blacks, onions and mesoporous micro-beads (Caldero-Moreno et al., 2005; Deshmukh et al., 2010). The spheres and balls can be hollow or solid and in this Chapter, spheres and balls will mean the same thing.

This is a continuation of the experimental work discussed earlier in section 3.1. As can be seen in Table 2, the higher acetylene flow rate and low temperature (900°C) tend to favour

production of CNBas. Figure 11 shows a TEM image of CNBas obtained at hydrogen flow rate of 118 ml/min and above, and constant acetylene flow rate of 370 ml/min at the decomposition temperature of 900°C as shown in Table 2. The CNBas, instead of CNTs, were formed because of low residence time and scattered catalyst particles resulting from high gaseous flow rates. Scattered catalyst particles led to 'growth-sites starvation'. These CNBas were also found to contain negligible traces of amorphous carbon and catalyst.

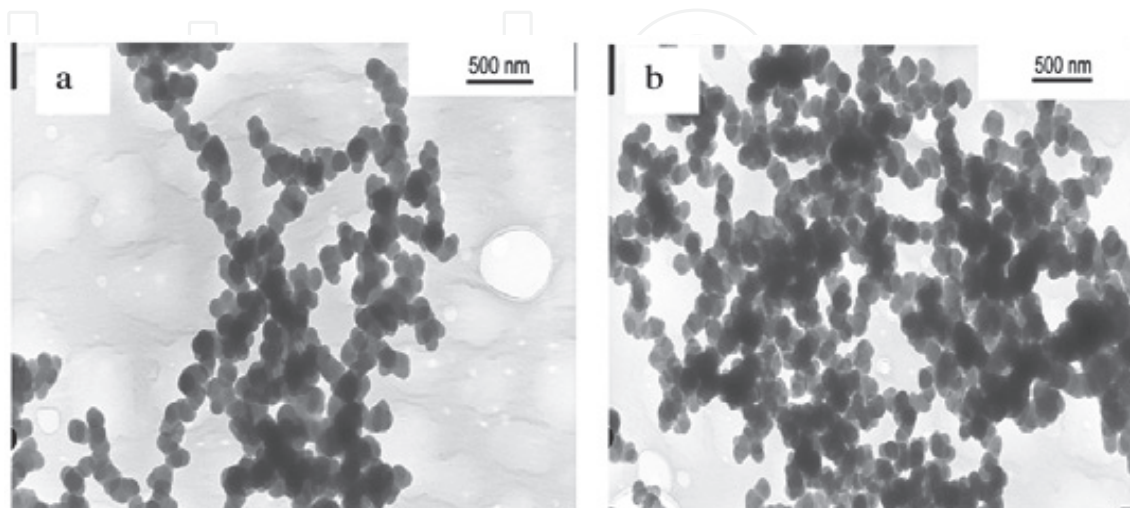


Fig. 11. TEM images of pure CNBas produced at (a) 900°C, $C_2H_2 = 370$ ml/min, $H_2 = 181$ ml/min (b) 900°C, $C_2H_2 = 370$ ml/min, $H_2 = 248$ ml/min (Afolabi et al., 2007).

In other related work, CNBas were only formed at temperatures of 1000°C and above in the absence of catalysts (Iyuke et al., 2009). This shows that temperature was paramount in the production of CNBas without the use of catalysts. The sufficiently enlarged TEM images showed that the diameter of the CNBa depended on gas flow rate ratios (i.e., acetylene: argon). Higher ratios tended to synthesise CNBas with smaller diameters while lower ratios produced CNBas with larger diameters. In other words, as the flow rate of acetylene increased, the size of CNBas decreased, and vice-versa. This observation relates the size of the CNBas to the residence time of acetylene in the reactor. The residence time of acetylene will be higher at the lower flow rate of acetylene and this will allow the products to grow further before exiting with carrier gas into the cyclones. Results also showed that the CNBa size increases as the pyrolysis temperature increases (Mhlanga et al., 2010).

The CNBas were also observed in experimental test-works performed in section 3.4. The CNBas were obtained at very low concentrations of ferrocene (e.g., 2%) and a pyrolysis temperature of 900°C. These CNBas were formed due to a low content of ferrocene at low pyrolysis temperature, as reported by Liu et al. (2002). The xylene might have assisted in the formation of these CNBas since low catalyst content at high temperature is known to result in CNTs with a high content of amorphous impurities (Afolabi et al., 2009).

4.2 Diamond films

The production of diamond films followed the experimental procedure in section 3.4. At an acetylene flow rate of 248 ml min⁻¹, hydrogen flow rate of 181 ml min⁻¹ and pyrolysis temperatures between 1000°C and 1100°C, diamond particles as well as glassy carbon were produced alongside CNTs (Afolabi et al., 2009). The diamond films were, however, thermodynamically unstable as they disappeared after a few minutes. The production of these

diamond particles (Figure 12) could be attributed to the nucleation by already produced CNTs in the reactor. This can be explained as follows (Hou et al., 2002); first it must be noted that diamond and CNTs – both being allotropes of carbon – have some structural resemblances. Under the conditions that were prevailing in the reactor, especially in the presence of hydrogen, the CNTs were broken into pieces lengthwise forming carbon nano-onions. The sp^3 bonds at the broken ends of the tubes turn to dangling bonds. Furthermore, due to the action of hydrogen and high temperature, the sp^2 bonds at the middle of the tubes between two ends can open and turn into sp^2 dangling bonds, and finally turn into sp^3 bonds again (Meilunas et al., 1991; Gruen et al., 1994). This results in countless heterogeneous nucleation sites, and the improvement of nucleation and growth for diamond.

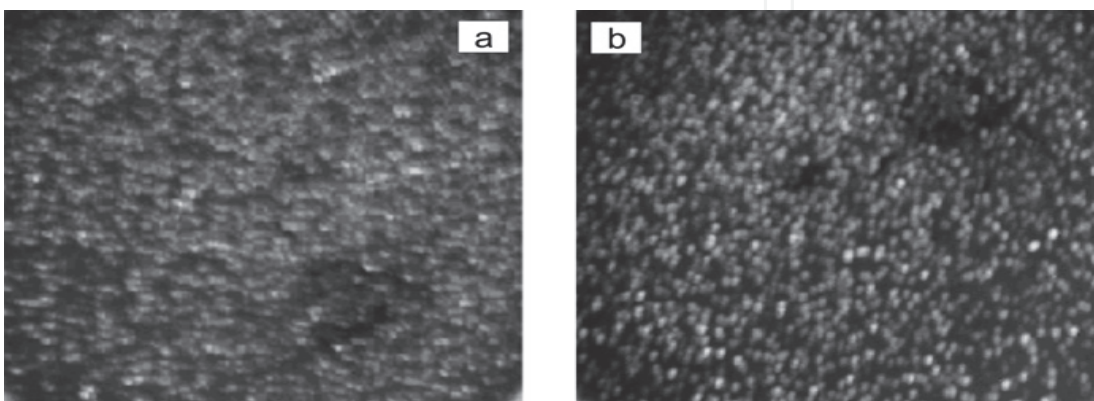


Fig. 12. Photographic images (EuroTEK 10 Megapixels) of diamond films obtained at (a) 10% ferrocene, 1000°C and a hydrogen flow rate of 118 ml min⁻¹, and (b) 10% ferrocene, 1100°C and a hydrogen flow rate of 181 ml min⁻¹ (Afolabi et al., 2009).

In the case of seeding with the low quality CNT mixture, the percentage of CNTs is very low (Hou et al., 2002). The separation action of hydrogen on CNT is weak. There are only few nano anion ends. So it is difficult for diamond to nucleate and grow while graphite film can grow and develop easily.

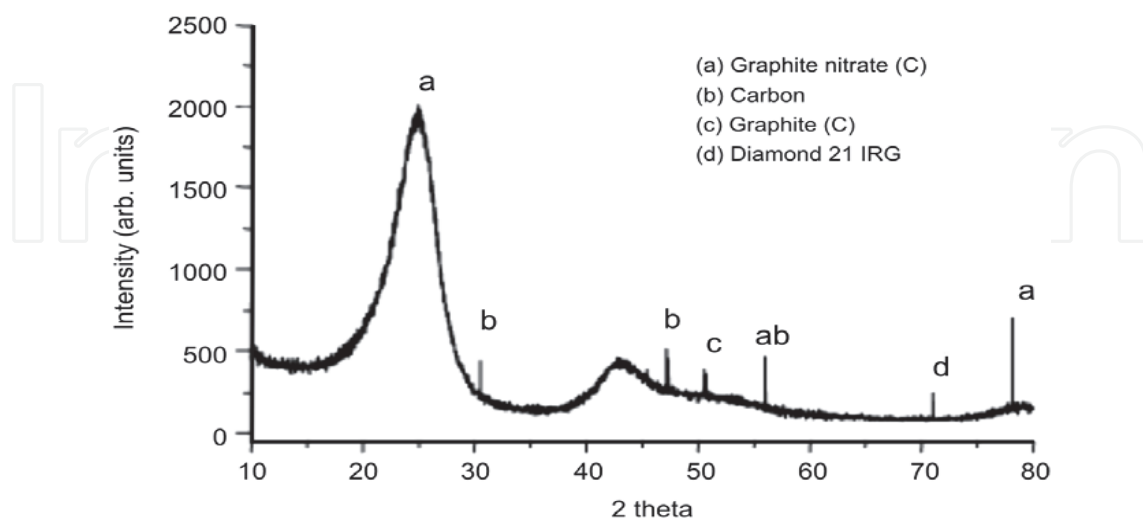


Fig. 13. X-ray diffraction analysis of a sample produced at 10% ferrocene, 1100°C, acetylene flow rate of 248 ml min⁻¹, and a hydrogen flow rate of 181 ml min⁻¹, confirming traces of diamond films (Afolabi et al., 2009).

Figure 13 shows the XRD analysis of the samples obtained at a temperature of 1100°C, an acetylene flow rate of 248 ml min⁻¹, hydrogen flow rate of 181 ml min⁻¹, and 10wt% concentrations of ferrocene, respectively (Afolabi et al., 2009). The analysis confirms the presence of diamond flakes and glassy carbon identified as graphite nitrate; the nitrogen in the nitrate may have been from the traces contained in the argon and hydrogen gases from the supplier, which were 4 and 2 volume per million (vpm), respectively. It was observed that the rate of production of diamond films increased with increases in the concentration of ferrocene, hydrogen flow rate and pyrolysis temperature.

5. Optimisation of the production of carbon nanomaterials

For practical commercial applications of CNTs, one would need quantities in the kilogram range (Subramoney, 1999). As a result, there is still a need to develop and optimise processing routes for the production of uniform and well defined carbon nanostructures in large quantities (Yu et al., 2005). We have seen in this Chapter that the production of carbon nanomaterials is variable, depending on interrelated controllable factors. Therefore, growth and optimisation of carbon nanomaterials need a targeted approach whereby parameters are tuned based on the type of nanomaterials required.

The huge number of parameters required in the growth process is a big challenge in the optimisation of as-produced carbon nanomaterials. However, we have seen that temperature and carbon source quantity are the important determinants in the production of carbon nanomaterials.

Figure 14 shows the effect of decomposition temperature and acetylene flow rate on the quantity of nanoparticles produced. The figure reveals that the quantity of nanoparticles produced increased with temperature and the flow rate of acetylene at constant flow rate of argon carrier gas of 181 ml/min. This indicates that at higher temperature, there is enough heat to effect the pyrolysis of acetylene leading to the formation of CNTs. The highest quantity of nanoparticles produced was obtained at temperature of 1050°C and

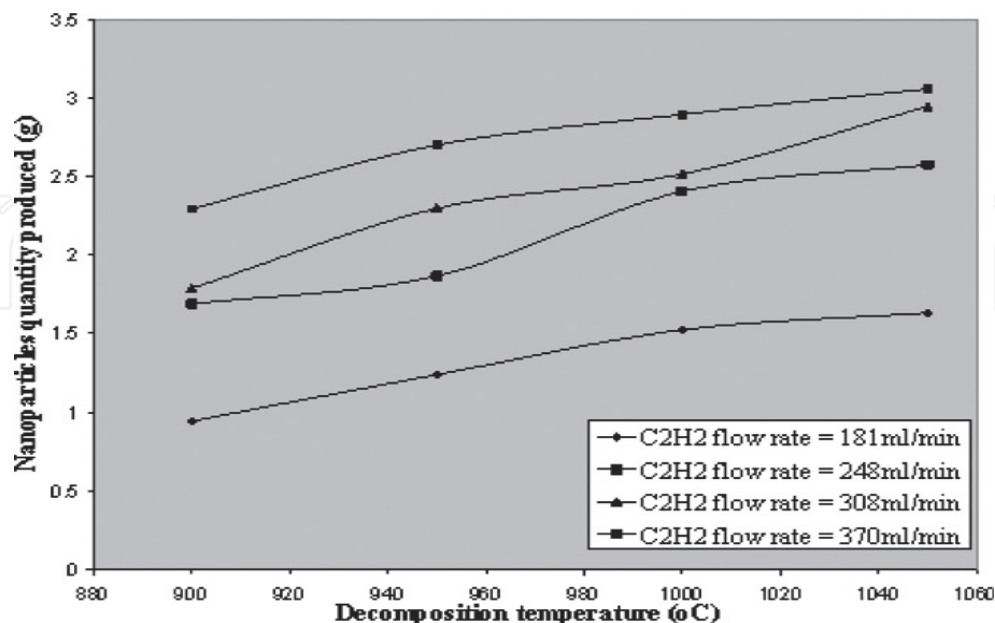


Fig. 14. Decomposition temperature versus quantity of nanoparticles produced at different flow rates of acetylene and constant hydrogen flow rate of 181 ml min⁻¹ (Afolabi et al., 2007).

acetylene flow rate of 370 ml/min. Even in the case of CNBa, the rate of production increased with increase in the feed stock flow rate at all pyrolysis temperatures (Mhlanga et al., 2010). However, at very high temperatures (results not shown here) there was a decrease in production rate. Furthermore, low values of amorphous carbon were observed as the temperature increased as a result of amorphous carbon burning off at high temperatures (Iyuke et al., 2007). In general, a higher temperature results in a modest increase in yield. Raman spectroscopy results presented in Figure 15 at different temperatures also shows that the crystallinity of CNTs produced depends on the pyrolysis temperature. The higher the temperature, the better the crystal structure of the CNTs.

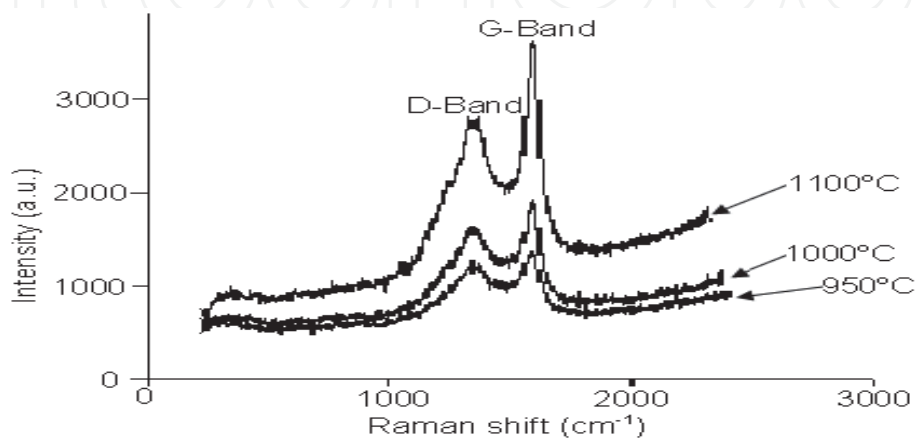


Fig. 15. Raman spectrometra of the CNTs sample produced (Abdulkareem et al., 2007; Iyuke et al., 2007).

Results obtained on the effect of temperatures on the rate of production of CNTs at different flow ratios of acetylene and hydrogen is shown in Figure 16 (Iyuke et al., 2006; Abdulkareem et al., 2007). It can be observed from the figure that the rate of production of CNTs at different flow ratios of acetylene and hydrogen is influenced significantly by the temperature. As the temperature increases, the rate of production of CNTs also increases as well as the quantity produced.

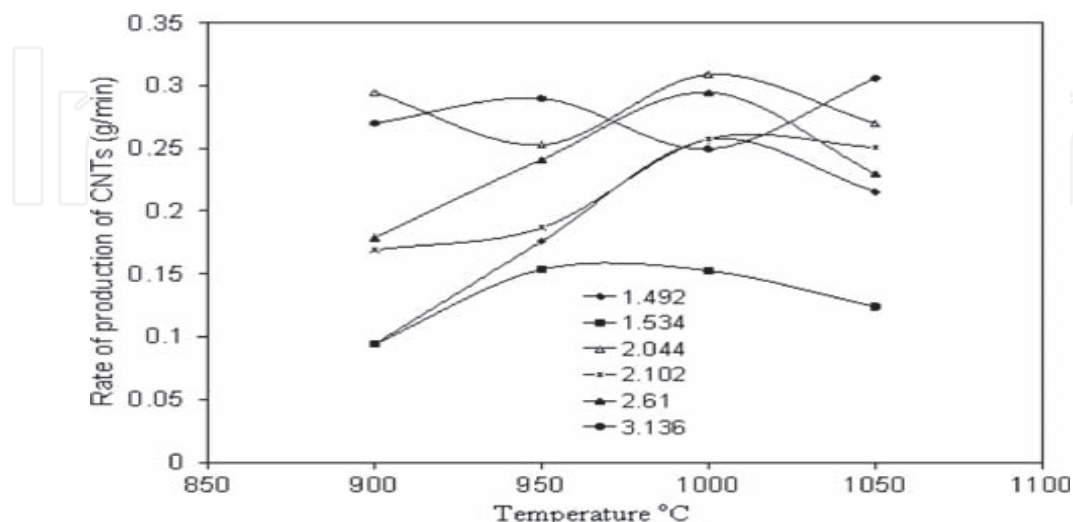


Fig. 16. Rate of production of CNTs at different temperatures and, flow ratios of acetylene to hydrogen (Iyuke et al., 2006; Abdulkareem et al., 2007).

Figure 16 also shows the effect of different flow ratios of acetylene to hydrogen at different temperatures. The figure shows that the rate of production initially increases with increase in C_2H_2/H_2 ratio at all temperatures. Different CNTs production rate peaks were observed for different C_2H_2/H_2 flow ratios at different temperatures. However, the highest CNTs production rate was observed at $1050^\circ C$ and this corresponds to C_2H_2/H_2 flow ratio of approximately 3 while the minimum CNTs production rate was obtained at flow ratio of 1.5 at $900^\circ C$. High quality and long CNTs were also obtained at C_2H_2/H_2 ratio of approximately equal to 3 and CNT production rate of 0.31 g/min (Iyuke et al., 2006; Abdulkareem et al., 2007). This shows the important role of the ratio of carbon source to hydrogen for good and high quality production of CNTs.

The effect of hydrogen flow rate on the rate of production of CNTs was also evaluated. At low flow rates (e.g., 118 – 181 ml/min), increases in flow rates increased the rate of CNT production (Abdulkareem et al., 2007; Iyuke et al., 2007). Here, hydrogen is not only required to create velocity profile in the reactor, but also takes part in the pyrolysis of acetylene. According to Kuwana et al. (2005), the three stages of reaction during pyrolysis of acetylene to give CNTs confirm the major role of hydrogen as shown in the equations below:



It can be observed from Equation 14 that the methane produced in Equation 13 decomposed at reactor temperature to produce CNTs and hydrogen. This reveals the positive influence of hydrogen in the production of CNTs.

However, it was seen that an increase in hydrogen flow rate above 181ml/min decreased the production rate monotonically from 4.2mg/s to zero (Abdulkareem et al., 2007; Iyuke et al., 2007). Reduction in rate of production of CNTs at higher hydrogen flow rate could be attributed to low residence time of acetylene in the reactor as a result of high velocity profile created by high hydrogen flow rate thereby suppressing the formation of CNTs. In other words, at high flow rate of hydrogen, the residence time of acetylene in the reactor becomes low because the hydrogen flow creates high velocity profile and push off the acetylene at a faster rate from the reaction zone. Singh et al. (2003) also made similar observations about the effect of hydrogen concentration on the production of CNTs using CVD technique. Apart from creating a velocity profile in the reactor, hydrogen may have also reduced ferrocene to atomic iron clusters or nanoparticles (Abdulkareem et al., 2007), thus making ferrocene inactive.

6. Conclusions, challenges and future prospects

CNTs (and other carbon nanomaterials) have reached the forefront of many industrial research projects since their rediscovery. However, there is still a great deal of work to be done for the full potential of CNTs to be fully realised. We have seen in this Chapter that various carbon nanomaterials can be prepared in an SFCCVD by careful controlling of parameters such as temperature and flow rates of carbon source and carrier gas. More importantly, the studies in this Chapter have clearly demonstrated that the SFCCVD method could be scaled up for continuous or semi-continuous production of carbon nanomaterials.

Though we have managed to produce CNTs and various other carbon nanomaterials in larger quantities, there are several challenges which need to be overcome before they can be widely used. They need to be synthesized in longer lengths, and improved techniques are required to align and evenly distribute them. Commercially available nanotubes are usually 0.5–5 μm long. In the design of conventional composites, for example, it is well known that the fiber length has a major influence on strengthening and stiffening of the matrix. For effective load transfer, the fiber length has to exceed a certain critical length, l_c , given by the following equation (Esawi & Faragi, 2007):

$$l_c = \sigma_f d / 2\tau_c \quad (15)$$

Where σ_f is the ultimate or tensile strength of the fiber, d is the fiber diameter and τ_c is the fiber-matrix bond strength. If the fiber length is less than l_c , the matrix cannot effectively grip the fibers and as a result they will slip.

The difficulty of dispersing the CNTs due to the fact that they tend to stick together and the difficulty of aligning the tubes are also major challenges. Although such issues have not yet been completely resolved, extensive efforts are underway to overcome them.

Researchers also agree that one of the major obstacles to using CNT is cost (Breuer & Sundararaj, 2004). Generally, the synthesis techniques used for making nanotubes are expensive. High quality/high purity CNTs could cost \$800/g and even ones with defects and impurities (metal catalyst and amorphous carbon) could cost \$5–35/g (Esawi & Farag, 2007).

Due to the great importance of CNTs, it is clear that novel technologies will emerge in future. It is also expected that more applications of CNTs will be found as some of their unknown unique properties are discovered.

7. References

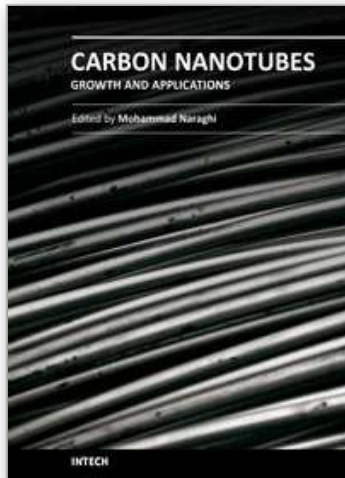
- Abdulkareem, A. S., Afolabi, A. S., Iyuke, S. E. & Piennar, C. H. vZ. (2007). Synthesis of carbon nanotubes by swirled floating catalyst chemical vapour deposition method, *Journal of Nanoscience and Nanotechnology* 7(10): 1-6.
- Afolabi, A. S., Abdulkareem, A. S. & Iyuke, S. E. (2007). Synthesis of carbon nanotubes and nanoballs by swirled floating catalyst chemical vapour deposition method, *Journal of Experimental Nanoscience* 2(4): 269-277.
- Afolabi, A. S., Abdulkareem, A. S. & Iyuke, S. E. (2009). Continuous production of carbon nanotubes and diamond films by swirled floating catalyst chemical vapour deposition method, *South African Journal of Science* 105: July/August.
- Agboola, A. E., Pike, R. W., Hertwig, T. A. & Lou, H. H. (2007). Conceptual design of carbon nanotube processes, *Clean Technologies and Environmental Policy* 9: 289-311.
- Ajayan, P.M. (2000). Carbon nanotubes, In: Nalwa, H.S. (ed.), *Handbook of nanostructured materials and nanotechnology*, Academic Press, Inc., New York, Vol. 5, pp 375 - 403.
- Amama, P. B., Pint, C. L., McJilton, L., Kim, S. M., Stach, E. A., Murray, P. T., Hauge, R. H. & Maruyama, B. (2009). Role of Water in super growth of single-walled carbon nanotube carpets, *Nano Letters* 9: 44-49.
- Bower, C., Zhou, O., Zhu, W., Werder, D.J. & Jin, S. (2000). Nucleation and growth of carbon nanotubes by microwave plasma chemical vapor deposition, *Applied Physics Letters* 77(17):2767-2769.

- Breuer, O. & Sundararaj, U. (2004). Big returns from small fibers: a review of polymer/carbon nanotube composites, *Polymer Composites* 25(6): 630–645.
- Caldero-Moreno, J. M., Labarta, A., Batlle, X., Pradell, T., Crespo, D & Thien Binh, V. (2005). Magnetic properties of dense carbon nanospheres prepared by chemical vapor deposition, *Chemical Physics Letters* 447: 295–299.
- Ci, L., Wei, J., Wei, B., Liang, J., Xu, C. & Wu, D. (2001). Carbon nanofibers and single-walled carbon nanotubes prepared by the floating catalyst method, *Carbon* 39(3): 329–335.
- Coleman, K. S. (2008). Nanotubes, *Annual Reports on the Progress of Chemistry, Section A: Inorganic Chemistry* 104: 379–393.
- Dai, H. (2001). Nanotube growth and characterisation, In: Dresselhaus, M. S., Dresselhaus, G., Avouris, P. (eds.), *Carbon Nanotubes: Synthesis, Structure, Properties and Applications*, Springer, New York, pp 29–51.
- Dai, H. (2002). Carbon nanotubes: opportunities and challenges, *Surface Science* 500: 218–241.
- Deshmukh, A. A., Mhlanga, S. D. & Coville, N. J. (2010). Carbon spheres, *Materials Science and Engineering Review* 70 (1–2): 1–28.
- de Jong, K. P. & Geus, J. W. (2000). Carbon nanofibers: catalytic synthesis and applications, *Catalysis Review* 42(4):481–510.
- Dresselhaus, M. S., Dresselhaus, G., Avouris, P. (eds.)(2001). *Carbon Nanotubes: Synthesis, Structure, Properties and Applications*, Springer, New York.
- Ducati, C., Alexandrou, I., Chhowalla, M., Robertson, J. & Amaratunga, G.A.J.(2004). The role of the catalytic particle in the growth of carbon nanotubes by plasma enhanced chemical vapor deposition, *Journal of Applied Physics* 95(11):6387–6391.
- Endo, M. (1988). Grow carbon-fibers in the vapor-phase, *Chemtech* 18(9): 568–576.
- Endo, M., Kim, Y. A., Hayashi, T., Nishimura, K. & Matusita, T. (2001). Vapour grown carbon fibres (VGCFs): basic properties and their battery applications, *Carbon* 39: 1287–1297.
- Eres, G., Kinkhabwala, A. A., Cui, H., Geohegan, D. B., Poretzky, A. A. & Lowndes, D. H. (2005). Molecular beam-controlled nucleation and growth of vertically aligned single-wall carbon nanotube arrays, *Journal of Physical Chemistry B* 109: 16684–16694.
- Esawi, A. M. K. & Farag, M. M. (2007). Carbon nanotube reinforced composites: Potential and current challenges, *Materials and Design* 28: 2394–2401.
- Fogler, H. C. (2006). *Elements of Chemical Reaction Engineering*, 4th Edition, Pearson Education, New Jersey.
- Gohier, A., Ewels, C.P., Minea, T.M. & Djouadi, M.A. (2008). Carbon nanotube growth mechanism switches from tip- to base-growth with decreasing catalyst particle size, *Carbon* 46: 1331–1338.
- Gommes, C., Blacher, S., Bossuot, Ch., Marchot, P., Nagy, J. B. & Pirard, J-P. (2004). Influence of the operating conditions on the production rate of multi-walled carbon nanotubes in a CVD reactor, *Carbon* 42: 1472–1482.
- Gruen, D. M., Liu, S., Krauss, A. R., Pan, X. (1994). Buckyball microwave plasma fragmentation and diamond-film growth, *Journal of Applied Physics* 75(3): 1758–1763
- Hofmann, S., Csányi, G., Ferrari, A.C., Payne, M.C. & Robertson, J. (2005). Surface diffusion: the low activation energy path for nanotube growth, *Physical Review Letters* 95 (036101):1–4.
- Hou, Y. Q., Zhuang, D. M., Zhang, G., Wu, M. S. & Liu, J. J. (2002). Preparation of diamond films by hot filament chemical vapour deposition and nucleation by carbon nanotubes, *Applied Surface Science* 185: 303–308.
- Iijima, S. (1991). Helical microtubules of graphitic carbon, *Nature* 354: 56–58.

- Iyuke, S.E., Piennar, C. H. vZ., Abdulkareem, A. S. & Afolabi, A. S. (2006). Optimising carbon nanotubes continuous production in a swirled fluid chemical vapour deposition reactor, In: *SACE 2006*, Available from <http://uir.unisa.ac.za/bitstream/10500/3261/1/abdulkareem.pdf>
- Iyuke, S. E. (2007). A process for production of carbon nanotubes, PCT Application WO2007/026213 (Published 2007/03/08) priority data ZA 2005/03438 2005/08/29.
- Iyuke, S.E., Abdulkareem, A. S., Afolabi, A. S. & Piennar, C. H. vZ. (2007). Catalytic production of carbon nanotubes in a swirled fluid chemical vapour deposition reactor, *International Journal of Chemical Reactor Engineering* 5(Note S5):1-9.
- Iyuke, S.E., Mamvura, T. A., Liu, K., Sibanda, V., Meyyappan, M. & Varadan V. K. (2009). Process synthesis and optimization for the production of carbon nanostructures, *Nanotechnology* 20:375602-375611.
- Jacques, D., Villain, S., Rao, A.M., Andrews, R., Derbyshire, F., Dickey, E.C. & Qian, D. (2000). Synthesis of multiwalled carbon nanotubes, *Materials Research Society* 593: 15-20.
- Journet, C. & Bernier, P. (1998). Production of carbon nanotubes, *Applied Physics A* 67: 1-9.
- Journet, C., Maser, W. K., Bernier, P., Loiseau, A., Lamy de la Chapelle, M., Lefrant, S., Denlard, P., Lee, R. & Fischer, J. E. (1997). Large-scale production of single-walled carbon nanotubes by the electric arc discharge, *Nature* 388: 756-758.
- Kim, K., Kim, K. J., Jung, W.S., Bae, S.Y., Park, J., Choi, J. & Choo, J. (2005). Chemical Investigation on the Temperature Re-dependent Growth rate of Carbon Nanotubes using Chemical Vapour Deposition of Ferrocene and Acetylene, *Chemical Physics Letters* 40:459-469.
- Kunadian, I., Andrews, R., Mengüç, M. P. & Qian, D. (2008). Multiwalled carbon nanotube deposition profiles within a CVD reactor: An experimental study, *Chemical Engineering Science* 64(7): 1503-1510.
- Kumar, M. & Ando, Y. (2005). Controlling the diameter of carbon nanotubes grown from camphor on a zeolite support, *Carbon* 43: 533-540.
- Kuwana, K., Endo, H., Saito, K., Qian, D., Andrews, R. & Grulke, E. A. (2005). Catalyst deactivation in CVD synthesis of carbon nanotubes, *Carbon* 43: 253 – 260.
- Kuwana, K. & Saito, K. (2007). Modeling ferrocene reactions and iron nanoparticle formation: application to CVD synthesis of carbon nanotubes, *Proceedings of the Combustion Institute* 31(2): 1857-1864.
- Lee, S. J., Baik, H. K., Yoo, J. & Han, J. H. (2002). Large scale synthesis of carbon nanotubes by plasma rotating arc discharge technique, *Diamond and Related Materials* 11: 914-917.
- Leonhardt, A., Hampel, S., Müller, C., Mönch, I., Koseva, R., Ritschel, M., Elefant, D., Biedermann, K. & Büchner, B. (2006). Synthesis, Properties, and Applications of Ferromagnetic-Filled Carbon Nanotubes, *Chemical Vapor Deposition* 12(6): 380-387.
- Levenspiel, O. (1999). *Chemical Reaction Engineering*, 3rd Edition, John Wiley and Sons, New York.
- Lewis, K. E. & Smith, G. P. (1984). Bond dissociation energies in ferrocene, *Journal of the American Chemical Society* 106: 4650-4651.
- Liu, Y., Hu, W., Wang, X., Long, C., Zhang, J., Zhu, D., Tang, D. & Xie S. (2000). Carbon nanorods, *Chemical Physics Letters* 331: 31-34.
- Liu, X.Y., Huang, B.C. & Coville, N. J. (2002). The Fe(CO)₅ catalyzed pyrolysis of pentane: carbon nanotubes and carbon nanoballs formation, *Carbon* 40: 2791-2799.
- Liu, R. (2008). The functionalisation of carbon nanotubes, PhD Thesis, University of New South Wales, Australia.

- Maphutha, S. (2009). Thermodynamic study of carbon nanotube production from greenhouse gases during syngas synthesis, MSc Dissertation, University of the Witwatersrand.
- Meilunas, R., Chang, R.P.H., Liu, S.Z. & Kappes, M. (1991). Nucleation of diamond films on surfaces using carbon clusters, *Applied Physics Letters* 59(26): 3461-3463.
- Mhlanga, S. D., Coville, N. J., Iyuke, S. E., Afolabi, A. S., Abdulkareem, A. S. & Kunjuzwa, N (2010). Controlled syntheses of carbon spheres in a swirled floating catalytic chemical vapour deposition vertical reactor, *Journal of Experimental Nanoscience* 5(1): 40-51.
- Merkoci, A. (2006). Carbon nanotubes in analytical sciences, *Microchimica Acta* 152(3-4):157-174.
- Meyyappan, M. (2004). *Growth: CVD and PECVD. Carbon nanotubes: science and applications*, CRC Press, Boca Raton
- Moisala, A., Nasibulin, A. G. & Kauppinen, E. I. (2003). The role of metal nanoparticles in the catalytic production of single-walled carbon nanotubes - a review, *Journal of Physics: Condensed Matter* 15: S3011-S3035.
- Moisala, A., Nasibulin, A. G., Brown, D. P. & Jiang, H. (2006). Single-walled carbon nanotube synthesis using ferrocene and iron pentacarbonyl in a laminar flow reactor, *Chemical Engineering Science* 61: 4393-4402
- Monthieux, M. & Kuznetsov, V. L. (2006). Who should be given the credit for the discovery of carbon nanotubes?, *Carbon* 44: 1621-1623
- Moothi, K. (2009). Carbon nanotube production from greenhouse gases during syngas synthesis, MSc Dissertation, University of the Witwatersrand.
- Nolan, P. E., Schabel, M. J., Lynch, D. C. & Cutler, A. H. (1995). Hydrogen control of carbon deposit morphology, *Carbon* 33: 79-85.
- Paradise, M. & Goswami, T. (2007). Carbon nanotubes - Production and industrial applications, *Materials and Design* 28:1477-1489.
- Qian, W., Wei, L., Cao, F., Chen, Q. & Qian, W. (2006). Low temperature synthesis of carbon nanospheres by reducing supercritical carbon dioxide with bimetallic lithium and potassium, *Carbon* 44(7): 1298-1352
- Robertson, J. 2004. Realistic applications of CNTs, *Materials Today* 7(10): 46-52
- Saito, Y. (1995). Nanoparticles and filled nanocapsules, *Carbon* 33:979-988.
- See, C.H. & Harris, A. T. (2007). A review of carbon nanotube synthesis via fluidized-bed chemical vapour deposition, *Industrial and Engineering Chemistry Research* 46(4): 997-1012.
- Simate, G. S., Iyuke, S. E., Ndlovu, S., Yah, C. S. & Walubita, L. F. (2010). The production of carbon nanotubes from carbon dioxide: challenges and opportunities, *Journal of Natural Gas Chemistry* 19(5): 453-460.
- Singh, C., Shaffer, M. S. P. & Windle, A. H. (2003). Production of controlled architectures of aligned carbon nanotubes by an injection chemical vapour deposition method, *Carbon* 41(2):359-368.
- Sinnott, S.B., Andrews, R., Qian, D., Rao, A. M., Mao, Z., Dickey, E. C. & Derbyshire, F. (1999). Model of carbon nanotube growth through chemical vapour deposition, *Chemical Physics Letters* 315: 25-30.
- Snoeck, J.W., Froment, G. F. & Fowles, M. (1997). Filamentous carbon formation and gasification: Thermodynamics, driving force, nucleation, and steady-state growth, *Journal of Catalysis* 169: 240-249.

- Soneda, Y., Duclaux, L. & Béguin, F. (2002). Synthesis of high quality multi-walled carbon nanotubes from the decomposition of acetylene on iron-group metal catalysts supported on MgO, *Carbon* 40(6): 965–969.
- Song, I.K., Cho, Y.S., Choi, G.S., Park, J.B. & Kim, D.J. (2004). The growth mode change in carbon nanotube synthesis in plasma-enhanced chemical vapor deposition, *Diamond and Related Materials* 13(4-8):1210–1213.
- Subramoney, S. (1999). Carbon nanotubes – a status report, *Interface* 8: 34–37.
- Tsoufis, T., Xidas, P., Jankovic, L., Gournis, D., Saranti, A., Bakas, T. & Karakassides, M. A. (2007). Catalytic production of carbon nanotubes over Fe-Ni bimetallic catalysts supported on MgO, *Diamond and Related Materials* 16(1): 155–160.
- Vivekchand, S.R.C., Cele, L.M., Deepak, F.L., Raju, A.R. & Govindaraj, A. (2004). Carbon nanotubes by nebulized spray pyrolysis, *Chemical Physics Letters* 386: 313–318.
- Winterbottom, J. M. & King, M. B. (eds.) (1999). *Reactor Design for Chemical Engineers*, Stanley Thornes (Publishers) Ltd, Gloucestershire.
- Wood, R. F., Pannala, S., Wells, J. C., Poretzky, A. A. & Geohegan, D. B. (2007). Simple model of the interrelation between single- and multiwall carbon nanotube growth rates for the CVD process, *Physical Review B* 75: 235446–235459.
- Xiang, R., Einarsson, E., Okawa, J., Miyauchi, Y. & Maruyama, S. (2009). Acetylene-accelerated alcohol catalytic chemical vapor deposition growth of vertically aligned single-walled carbon nanotubes, *Journal of Physical Chemistry C* 113: 7511–7515.
- Yah, C. S., Iyuke, S.E., Simate, G. S., Unuabonah, E. I., Bathgate, G., Matthews, G. & Cluett, J.D. (2011). Continuous synthesis of multiwalled carbon nanotubes from xylene using the swirled floating catalyst chemical vapour deposition technique, *Journal of Materials Research* 26(5): 640–644.
- Yamada, T., Maigne, A., Yudasaka, M., Mizuno, K., Futaba, D. N., Yumura, M., Iijima, S. & Hata, K. (2008). Revealing the secret of water-assisted carbon nanotube synthesis by microscopic observation of the interaction of water on the catalysts, *Nano Letters* 8: 4288–4292.
- Yang, K. L. & Yang, R. T. (1986). The accelerating and retarding effects of hydrogen on carbon deposition on metal surfaces, *Carbon* 24 (6): 687–693.
- Yoon, Y.J. & Baik, H. K. (2001). Catalytic growth mechanism of carbon nanofibers through chemical vapour deposition, *Diamond and Related Materials* 10: 1214–1217.
- Young, J. L. & DeSimone, J. M. (2000). Frontiers in green chemistry utilising carbon dioxide for polymer synthesis and applications, *Pure and Applied Chemistry* 72(7): 1357–1363.
- Yu, Z., Chen, D., Tøtdal, B., Zhao, T., Dai, Y., Yuan, W. & Holmen, A. (2005). Catalytic engineering of carbon nanotube production, *Applied Catalysis A: General* 279: 223–233.
- Zhang, F., Shen, J., Sun, J. & McCartney, D. G. (2006). Direct synthesis of diamond from low purity carbon nanotubes, *Carbon* 44(14): 3136–3138.
- Zhong, Z., Chen, H., Tang, S., Ding, J., Lin, J. & Tan, K. L. (2000). Catalytic growth of carbon nanoballs with and without cobalt encapsulation, *Chemical Physics Letters* 330: 41–47.
- Zhong, G., Hofmann, S., Yan, F., Telg, H., Warner, J. H., Eder, D., Thomsen, C., Milne, W. I. & Robertson, J. (2009). Acetylene: A key growth precursor for single-walled Carbon nanotube forests, *Journal of Physical Chemistry C* 113: 17321–17325.



Carbon Nanotubes - Growth and Applications

Edited by Dr. Mohammad Naraghi

ISBN 978-953-307-566-2

Hard cover, 604 pages

Publisher InTech

Published online 09, August, 2011

Published in print edition August, 2011

Carbon Nanotubes are among the strongest, toughest, and most stiff materials found on earth. Moreover, they have remarkable electrical and thermal properties, which make them suitable for many applications including nanocomposites, electronics, and chemical detection devices. This book is the effort of many scientists and researchers all over the world to bring an anthology of recent developments in the field of nanotechnology and more specifically CNTs. In this book you will find:

- Recent developments in the growth of CNTs
- Methods to modify the surfaces of CNTs and decorate their surfaces for specific applications
- Applications of CNTs in biocomposites such as in orthopedic bone cement
- Application of CNTs as chemical sensors
- CNTs for fuelcells
- Health related issues when using CNTs

How to reference

In order to correctly reference this scholarly work, feel free to copy and paste the following:

Sunny E. Iyuke and Geoffrey S. Simate (2011). Synthesis of Carbon Nanomaterials in a Swirled Floating Catalytic Chemical Vapour Deposition Reactor for Continuous and Large Scale Production, Carbon Nanotubes - Growth and Applications, Dr. Mohammad Naraghi (Ed.), ISBN: 978-953-307-566-2, InTech, Available from: <http://www.intechopen.com/books/carbon-nanotubes-growth-and-applications/synthesis-of-carbon-nanomaterials-in-a-swirled-floating-catalytic-chemical-vapour-deposition-reactor>

INTECH
open science | open minds

InTech Europe

University Campus STeP Ri
Slavka Krautzeka 83/A
51000 Rijeka, Croatia
Phone: +385 (51) 770 447
Fax: +385 (51) 686 166
www.intechopen.com

InTech China

Unit 405, Office Block, Hotel Equatorial Shanghai
No.65, Yan An Road (West), Shanghai, 200040, China
中国上海市延安西路65号上海国际贵都大饭店办公楼405单元
Phone: +86-21-62489820
Fax: +86-21-62489821

© 2011 The Author(s). Licensee IntechOpen. This chapter is distributed under the terms of the [Creative Commons Attribution-NonCommercial-ShareAlike-3.0 License](#), which permits use, distribution and reproduction for non-commercial purposes, provided the original is properly cited and derivative works building on this content are distributed under the same license.

IntechOpen

IntechOpen